

# Glitching Pulsars: Unraveling the Interactions of General Relativistic and Quantum Fields in the Strong Field Regimes

Ahmad A. Hujeirat<sup>1</sup>, Ravi Samtaney<sup>2</sup>

<sup>1</sup>IWR, Universität Heidelberg, Heidelberg, Germany

<sup>2</sup>Applied Mathematics and Computational Science, KAUST, Thuwal, Jeddah, KSA

Email: AHujeirat@uni-hd.de, ravi.samtaney@kaust.edu.sa

**How to cite this paper:** Hujeirat, A.A. and Samtaney, R. (2019) Glitching Pulsars: Unraveling the Interactions of General Relativistic and Quantum Fields in the Strong Field Regimes. *Journal of Modern Physics*, 10, 1696-1712.

<https://doi.org/10.4236/jmp.2019.1014111>

**Received:** November 27, 2019

**Accepted:** December 21, 2019

**Published:** December 24, 2019

Copyright © 2019 by author(s) and Scientific Research Publishing Inc. This work is licensed under the Creative Commons Attribution International License (CC BY 4.0).

<http://creativecommons.org/licenses/by/4.0/>



Open Access

---

## Abstract

In this article we modify our previous model for the mechanisms underlying the glitch phenomena in pulsars. Accordingly, pulsars are born with embryonic cores that are made of purely incompressible superconducting gluon-quark superfluid (henceforth SuSu-cores). As the ambient medium cools and spins down due to emission of magnetic dipole radiation, the mass and size of SuSu-cores must grow discretely with time, in accordance with the Onsager-Feynmann analysis of superfluidity. Here we argue that the space-time embedding glitching pulsars is dynamical and of bimetric nature: inside SuSu-cores the spacetime must be flat, whereas the surrounding region, where the matter is compressible and dissipative, the spacetime is Schwarzschild. It is argued here that the topological change of spacetime is derived by the strong nuclear force, whose operating length scales are found to increase with time to reach  $\mathcal{O}(1)$  cm at the end of the luminous lifetimes of pulsars. The here-presented model is in line with the recent radio- and gravitational wave observations of pulsars and merger of neutron stars.

## Keywords

Relativity: Numerical, General, Black Hole Physics, Magnetars, Neutron Stars, Pulsars, Superfluidity, Superconductivity, Gluons, Quarks, Quantum Chromodynamics (QCD)

---

## 1. Internal Structure of UCSs

Pulsars, neutron stars (NSs) and magnetars build the family of ultra-compact

stars (UCSs). This is a sub-class of the compact objects (COs), which, in addition, include white dwarfs (WDs) and black holes (BHs) as well. Unlike COs, the members of UCSs share the same evolution and may have the same cosmological fate. Our analysis here applies to UCSs but neither to WDs nor to BHs. The compactness parameter of UCSs,  $\alpha_s$ , is generally larger than half (see [1] [2] [3] and the references therein). Recalling that the average density of matter in the interiors of UCSs is larger than the nuclear one,  $\rho_0$ , then these objects are well-suited for probing the interaction of general relativity with quantum fields in the strong field regime (**Figure 1**).

In fact pulsars and NSs have been successfully used for probing general relativity, such as the emission of gravitational waves (GWs) in binary pulsars and direct detection GWs through merger of neutrons stars and black holes (see [4] and [5] for detailed reviews). However, the internal structure of UCSs will continue to be a mystery and remain a challenge for astrophysicists not for a short time (see the review in [6] and the references therein). On the other hand, the glitch-phenomena observed to associate pulsars [7] [8] are events that may be considered to be connected to the dynamics of matter inside their interiors (see [6] [7] [9] [10] and the references therein). However, based on observations and theoretical arguments, one may try to constrain the nature of matter inside normal UCSs as follows:

1) The observed continuous spin-down of UCSs results from the combined loss of magnetic and rotational energies (see [6] and the references therein). These are estimated to fall in the range:  $[10^{37}, 10^{40}]$  erg/s, depending on the nature and age of the concerned UCSs and specifically whether these concerned ones are magnetars, pulsars or neutron stars [9] [11]. This would imply complete exhaustion of the stored removable energies<sup>1</sup> inside pulsars within about ten million years, provided that the heat conductivity operates on length scales that are larger than the nuclear ones. Consequently, very old and isolated UCSs, including those formed through the collapse of the first generation of stars, must be dark by now and therefore excellent candidates for stellar black hole. This argument would explain why neither UCSs nor black holes have never been observed in the mass range  $[2M_{\odot} \leq \mathcal{M} \leq 5M_{\odot}]$ .

2) The rest of thermal, kinetic and magnetic energies that are left from the collapse of the progenitors of UCSs are transported outwards into the outer shells and subsequently liberated away. Due to the relatively small thermal energy content in UCSs and in the absence of nuclear energy generation, the Tolman-Oppenheimer-Volkoff equation (TOV-equation) may still accept a positive gradient of the thermal energy, turning the central core to the coldest region inside UCSs, thereby facilitating a phase transition of the compressible dissipative nuclear matter into incompressible superfluid (see [12] for further details on the properties of incompressible fluid flows). Such a phase transition may still occur even when the matter's temperature is still beyond several million degrees [11] (**Figure 2**).

<sup>1</sup>*i.e.* energies other than rest energy.

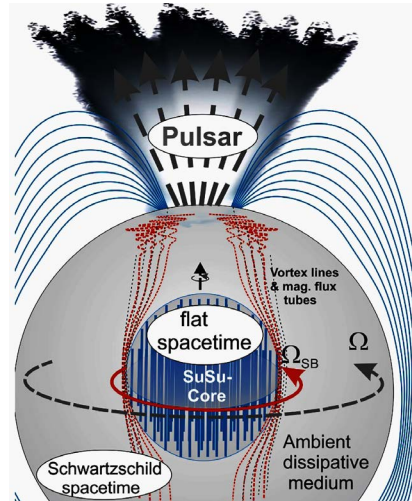


**Figure 1.** A schematic description of the internal structure of glitching pulsars. Pulsars are born with embryonic cores that are made of incompressible gluon-quark superfluids and embedded in flat spacetime. The overlying shells are made of dissipative and compressible quantum fluids, but embedded in Schwarzschild spacetime.

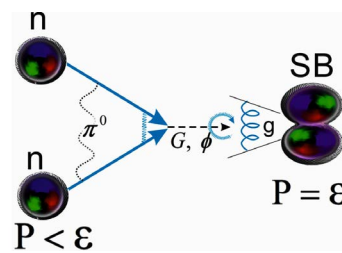


**Figure 2.** Neutron merger at the centers of pulsars. The compressible and dissipative neutron fluid is governed by EOSs in which  $P < \epsilon$ . When the density approaches the critical density,  $\rho_c$ , then the EOS changes into  $P = \epsilon$ , which corresponds to incompressible quantum fluid. At  $\rho = \rho_c$ , it is energetically favourable for neutrons to start deconfine the quarks and merge together to form an ocean of gluon-quark superfluid, though the resulting global gluon cloud must be much more energetic.

3) Theoretical studies show that in the regime of nuclear density and beyond, almost all EOSs used for modelling the state of matter in the interiors of UCSs tend to converge to the limiting case:  $\epsilon = P$  (see [9] and the references therein). However, this state corresponds to pure incompressible nuclear fluids [2]. Due to causality and stability reasons, incompressible nuclear fluids should be free of all other removable energies, such as thermal, kinetic and magnetic energies. Hence the core is expected to end up as a condensate with zero-entropy, whose constituents communicate with each other with the speed of light and therefore the momentum exchange between them must saturate around a universal maximum. In this case, the coupling constant in the context of asymptotic freedom in QCD would converge to its universal minimum value, where quarks inside merged-neutrons are allowed to oscillate locally [13] [14]. Such a zero-entropy superfluid<sup>2</sup> cannot accept spatial variations or stratification due to gravity and <sup>2</sup>Vanishing energy loss due to acceleration/deceleration should be excluded.

therefore the embedding spacetime ought to be flat. This state may be maintainable, if involved quarks are attached to a spatially fixed lattice, where they may behave collectively as a single macroscopic quantum entity.

Indeed, although both entropy and energy states of colliding protons at the RHIC and LHC differ significantly from those at the centers of UCSs, these experiments have shown that the properties of the resulting fluids mimic those of perfect fluids (see [15] [16] for further details).

4) Based on astronomical observations, there appears to be a gap in the mass spectrum of compact objects: neither black holes nor NSs have never been observed in the mass range  $[2M_{\odot} < \mathcal{M} < 5M_{\odot}]$ . Moreover, intensive astronomical observations of the newly detected NS-merger GW170817 [1] failed to unambiguously classify the nature of the remnant object, though theoretically it must be a stellar black hole. These both facts are in line with our scenario which predicts that massive pulsars should evolve on the cosmological time scale toward forming massive dark energy objects that become indistinguishable from stellar black holes. A schematic description of the scenario is shown in **Figure 1** **Figure 2** and **Figure 4**.

### 1.1. The Model and the Governing Equations

For modelling the internal structure of pulsars, the general relativistic field equations should be solved:

$$G_{\mu\nu} = \kappa T_{\mu\nu}, \quad \text{for } \mu, \nu : 0 \rightarrow 4, \quad (1)$$

where  $G_{\mu\nu}, T_{\mu\nu}$  are the Einstein and the Stress-Energy tensors, respectively, and  $\kappa$  is a coefficient (see [17] [18] for further details). The rotational, magnetic, thermal and other energies in UCSs are generally about three orders of magnitude smaller than the rest energy and therefore they may be safely neglected. In this case, Schwarzschild spacetime is most suited for modelling their internal structures. Hence the corresponding metric reads:

$$ds^2 = e^{2\nu(r)} dt^2 - e^{2\lambda(r)} dr^2 - r^2 d\Omega^2, \quad (2)$$

where  $d\Omega = d\theta^2 + \sin^2 \theta d\varphi^2$  is a surface element on a sphere of radius “ $r$ ”.

The field equations can then be reduced to just one single equation, *i.e.* to the so-called Tolman-Oppenheimer-Volkoff (TOV) equation:

$$\frac{dP}{dr} = -\frac{G}{c^4 r^2} \frac{[\varepsilon + P][m(r) + 4\pi r^3 P]}{1 - r_s/r}, \quad (3)$$

where  $r, r_s, G, P, m(r)$  correspond to the radius, Schwarzschild radius, gravitational constant, pressure and the dynamical mass, respectively (see Sec. (4) in [2] for further details).

Recalling that GR is incapable of modelling gravitationally bound incompressible matter, then the spacetime embedding pulsars may be decomposed into two separate domains: a flat spacetime that embeds the SuSu-core and a surrounding Schwartzschild spacetime that embeds the ambient media as mentioned above. The decomposition of the domain is motivated by relativistic cau-

sality which prohibits fluid stratification or spatial variation of the density of purely incompressible fluids; hence why the spacetime embedding the core must have zero-curvature, *i.e.* purely flat.

Based thereupon the line element in the core is described by the metric in spherical polar coordinates  $(t, r, \theta, \varphi)$ :

$$ds^2 = c^2 dt^2 - dr^2 - r^2 d\Omega^2. \tag{4}$$

The physical properties of the SuSu-core are set to affect the structure of the ambient medium by allowing  $m(r)$  and  $r_s$  in the TOV-equation to depend on the total enclosed mass, *i.e.* on  $m(r) = M_{SuSu} + 4\pi \int_{r=1}^{\infty} \rho r^2 dr$ .

On the other hand, as the matter in the rotating core is in incompressible superfluid state, it must contain a discrete array of vortices. Their total number,  $N$ , the mass and size growth of the core are determined through the Onsager-Feynmann equation for modelling quantized circulations:

$$\oint \mathbf{v} \cdot d\ell = \frac{2\pi\hbar}{m^*} N, \tag{5}$$

where  $v, \ell, \hbar, m^*, N$  correspond to rotational velocity, line-element along the circular path, the reduced Planck constant, the mass of the superfluid particles and the enclosed number of vortices, respectively [19] [20]

Inside the core, the quantum fluid is assumed to have zero-entropy and has reached the critical supranuclear density,  $\rho = 3\rho_0$ , beyond which merger of individual gluon clouds into a global one becomes possible.

The effective energy of the latter cloud correlates linearly with the number of merged neutrons, *i.e.*

$$\sum_1^N E_n^0 \xrightarrow{\text{mergering process}} \sum_1^N E_n^0 + N \times \Delta E_{bag}, \tag{6}$$

where  $\Delta E_{bag}$  is the bag energy enhancement needed to confine the quarks inside the super-baryon and  $N$  denotes the total number of merged neutrons to forming the super-baryon,  $E_n$  is the rest energy of a single neutron. In this case the energy and pressure of the incompressible gluon-quark superfluid inside the core read:  $\varepsilon_{tot} = \varepsilon_0 + \varepsilon_\phi$ ,  $P_{tot} = P_0 + P_\phi$ , where  $\varepsilon_0$  is the energy density of the baryonic matter and  $\varepsilon_\phi = \frac{1}{2}\dot{\phi}^2 + V(\phi) + \frac{1}{2}(\nabla\phi)^2$  and

$P_\phi = \frac{1}{2}\dot{\phi}^2 - V(\phi) + \frac{1}{6}(\nabla\phi)^2$  are the energy density and pressure of the scalar

field, which are assumed to be identical to  $\Delta E_{bag}$ . As the matter inside the cores of pulsars is set to be incompressible and stationary, it is reasonable to assume  $\phi = constant$ . In this case,  $\dot{\phi}$  and  $\nabla\phi$  must vanish and  $V(\phi)$  can be considered as the energy density required for deconfining the quarks inside the super-baryon, *i.e.*, the SuSu-core. Here we set  $\varepsilon_{tot} = 2\varepsilon_0$ , whereas the pressure  $P_{tot} = P_0 - V(\phi) = \varepsilon_0 - V(\phi) = 0$ . Thus the total local pressure of incompressible gluon-quark superfluid inside SuSu-cores vanishes completely. Exterior to the core, the matter is said to be baryonic, dissipative, compressible and embedded in a Schwarzschild spacetime.

### 1.1.1. Initial and Boundary Conditions

The present scenario is based on a previous model for the origin of glitches in pulsars. Accordingly, pulsars and young neutron stars are expected to undergo billions of glitch events during their luminous lifetimes before ending as ultra-compact and invisible dark energy objects.

In the present study, we select several epochs in the lifetimes of pulsars and the corresponding internal structures are calculated subject to the following conditions:

- ◆ The pulsar has the initial mass of  $1.33\mathcal{M}_\odot$ , which is made of a purely baryonic compressible matter.
- ◆ The pulsar is set to have initially the compactness parameter  $\alpha_s = 1/2$ .
- ◆ The central baryonic density is set to be equal to the critical  $\rho_c = 3\rho_0$ , at which a transition into quark-deconfinement occurs, and where the Gibbs function vanishes.
- ◆ The dissipative and compressible baryonic matter is set to obey the polytropic EOS:  $P = \mathcal{K}\rho^\gamma$ .

The selected models correspond to pulsar phases in which the enclosed SuSu-cores have reached the following radii:  $R_{SuSu} = 0.333, 0.525, 0.78525$  and  $0.8575$  in units of  $[\tilde{R}(=R_s/\alpha_s)]$ , where  $R_s$  is the corresponding Schwarzschild radius. The total density inside SuSu-cores amounts to:

$$\rho_{tot} = \rho_b + \rho_\phi = 2\rho_c \approx 6\rho_0.$$

1) Model-0: The pulsar is made of purely baryonic matter. Here, the TOV-equation is solved for the pressure starting from a given  $P(r=0) = P_0$  up to a radius, where the pressure vanishes.

2) Combined-models: The pulsar models are made both of SuSu-cores surrounded by dissipative and compressible quantum fluid. The radii of the cores here read:  $R_{SuSu} = 0.333, 0.525, 0.78525, 0.8575$ . The total mass of the core is calculated through the integration:

$$m_{tot}(r = R_{core}) = \int_0^{R_{core}} (\varepsilon_b + \varepsilon_\phi) dr. \quad (7)$$

The solutions here are based on adapting the parameters  $\mathcal{K}$  and  $\gamma$  of the EOS in such a manner so that the initial baryonic mass of  $1.33\mathcal{M}_\odot$  the pulsar remain preserved.

3) The ultimate final phase: Here the radius and mass of the SuSu-core are roughly equal to the critical values:  $R_{SuSu} = 0.859 \approx R_{Schw.}$  and  $M_{SuSu} \approx M_{Schw.}$ . Here the initial pulsar must have metamorphosed entirely into an invisible SuSu-object.

### 1.1.2. Results

For enhancing the spatial accuracy of the calculations, an explicit adaptive mesh refinement (EAMR) has been developed, in which the aspect ratio,  $dr_{max}/dr_{min}$ , may reach 100 million. Unlike self-adaptive mesh refinement (AMR), EAMR is based on a posteriori refining the grid distribution in certain locations of the domain, where the gradients of the physical variables are large. This may be

achieved by externally and manually manipulating the grid distribution and restarting the calculations anew. In the present case, for example, the location, where the pressure vanishes is vitally important and therefore the resolution should be maximally refined (Figure 3). Unlike AMR, solution methods based on EAMR generally converge much faster than their AMR-counterparts, hence contributing to the global efficiency and robustness of the numerical solution procedure (see [21] and the references therein).

Based on the previous study [22], five episodes in the cosmological evolution of pulsars have been selected (see Figure 4). For each episode, the TOV equation, modified to include dark energy input at the background of the here-presented bimetric scenario of spacetime, is solved.

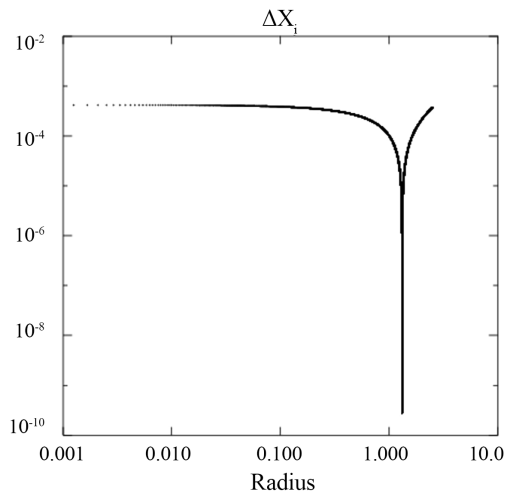


Figure 3. The distribution of the finite volume cells as function of radius. Here the explicit adaptive mesh refinement (EAMR) has been employed to increase the accuracy at both the interface between the core and the ambient medium as well as to outer radius of the object.

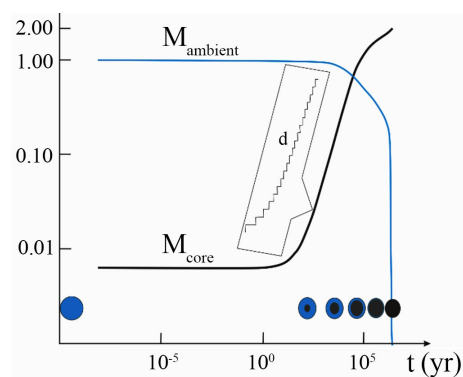


Figure 4. Based on the solution of the TOV equation in combination with Onsager-Feynmann equation, the size and mass of SuSu-cores grow with time following a well-defined mathematical sequence  $\{\alpha_c^n\}$ . The discrete increase of  $M_{core}$  is magnified and shown “d”. To verify the bimetric model of pulsars, six epochs with different core-sizes have been selected: a newly born pulsar, four intermediate phases and the final massive state, where the whole object turns into an invisible dark energy object.

In **Figure 5** and **Figure 6** the profiled of the corresponding five runs are displayed. Profile (1) corresponds to the radial distribution of the pressure obtained by solving the TOV equation. The phase here corresponds to the moment of birth of the pulsar, when it is entirely embedded in a Schwarzschild spacetime.

Profiles (2, 3, 4 and 5) in **Figure 5** show the radial distributions of the pressure at different epochs, specifically when the SuSu-core has grown in mass and size to reach the radii values:  $R_{SB} = 0.333, 0.525, 0.78525$  and  $0.7875$ .

Note that as the SuSu-core becomes more massive, the curvature of spacetime embedding the ambient medium is enhanced, which, in turn, compresses the ambient medium even more, thereby reducing the effective radius of the pulsar. This would explain the mass-radius relations displayed in **Figure 7** and **Figure 8**. Here the corresponding Schwarzschild radius increases and propagates outwards to finally meet the decreasing radius of the contacting pulsar. The overlapping of both radii is expected to occur at the end of the pulsar's luminous lifetime (see **Figure 4** and Profile 5 of **Figure 5**).

As purely incompressible superfluids in flat spacetime have zero-spatial variations (**Figure 9**), then the gravitational potential inside SuSu-cores should attain a sequence of constant values. Their magnitudes correlate with the mass and size of the SuSu-core. Consequently, as the SuSu-core becomes more massive, the gravitational redshift of the pulsar increases to finally reach very large values at the end of the pulsar's luminous lifetime (Profile "6" in **Figure 10**). Here the Schwarzschild radius becomes almost equal to the effective radius of the object, enforcing the object to sink deeply in spacetime to become invisible.

Note that the profiles shown in **Figure 9** and **Figure 10** are not just schematic representations, but have been obtained using direct numerical computations.

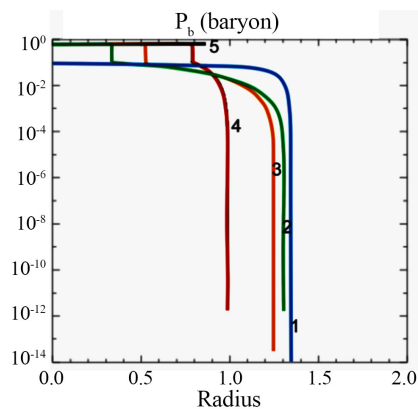


**Figure 5.** The distribution of the baryonic pressure inside an evolving pulsar after five selected glitch events at different epochs. Inside the core, in addition to the rest energy of the baryonic matter, there is an energy enhancement due to the scalar field, which is equivalent to the additional energy required for re-confining the sea of quarks. The transition between both regions is not smooth as the matter inside the core evolves quantum mechanically, whereas the ambient medium obeys the normal laws of continuum.

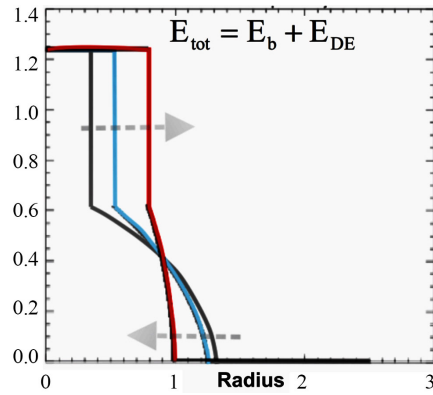


**Figure 6.** Similar to the previous figure: the distribution of the total energy density inside both the core and the ambient dissipative medium are shown.

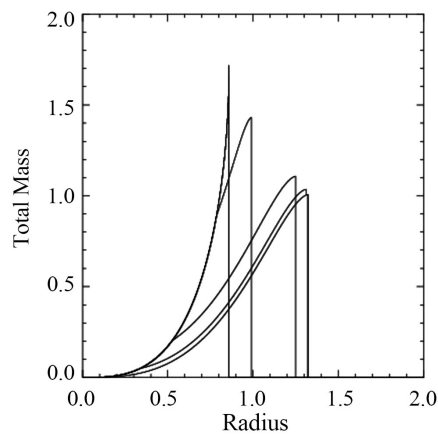


**Figure 7.** The total enclosed mass of the object versus radius after selected glitch events. As the mass of the SuSu-core increases, its compactness of the whole object increases as well to finally reach the critical Schwarzschild mass.

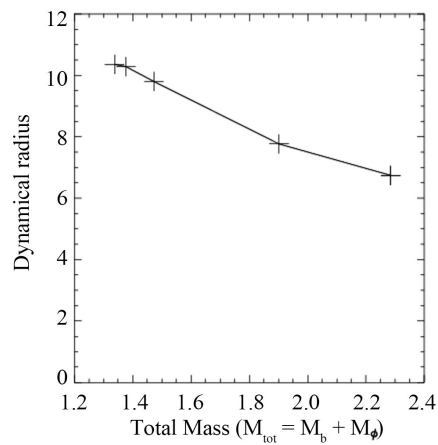


**Figure 8.** The mass-radius relation of an evolving pulsar after selected glitch events. As the core becomes more massive, the Schwarzschild radius grows and converges asymptotically to the effective radius of the entire contracting object.

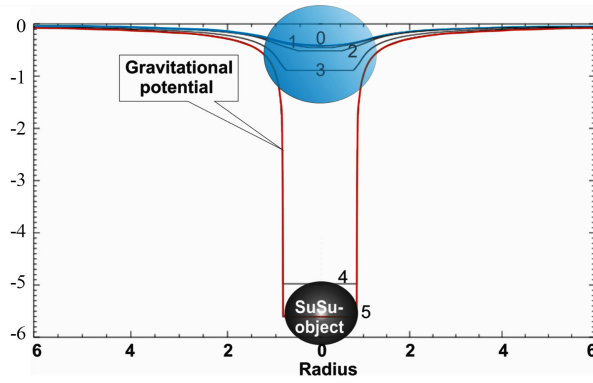


**Figure 9.** The radial distribution of the gravitational potential shown for different epochs in the lifetime of the pulsar, which is equivalent to the radial projection of spacetime inside the SuSu-core governed by Minkowski spacetime, as well as in the surrounding region governed by the Schwarzschild metric. Obviously, as the object become more massive, it sinks deeper in spacetime, becomes gravitational redshifted to finally ends as an invisible dark energy object.

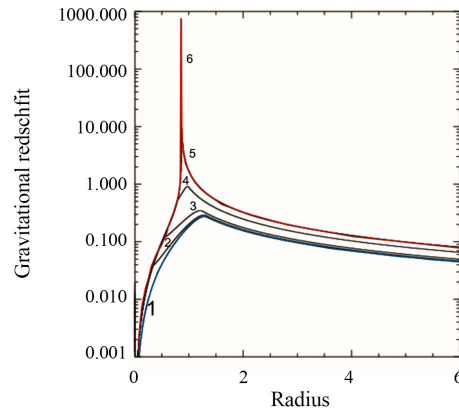


**Figure 10.** The radial distribution of the gravitational redshift ( $Z$ ) of the pulsar at different evolutionary epochs. Profile “1” corresponds to the low “ $Z$ ” immediately after the pulsar was born, whereas Profile “6” depicts the divergent limit of “ $Z$ ” at the surface of the object when it becomes completely invisible.

## 2. Summary and Discussion

The here-presented pulsar model is analogous to the terrestrial rotating superfluid Helium in a container. While the SuSu-matter inside the core corresponds to rotating superfluid Helium, the ambient dissipative medium would represent the solid container.

However, the pulsar model here is much more sophisticated, as quantum and general relativistic effects are taken into account. In the following, we discuss the main features of the model.

- For  $\rho \geq \rho_{crit}$ , neutrons at the center of pulsars are set to merge together to form an incompressible gluon-quark superfluid, governed by the critical EOS  $P = \varepsilon$ . This argument is supported by the following two observations:
  - ✧ Theoretical studies of nuclear interactions in the regime  $\rho \geq \rho_0$  show that almost all EOSs converge to the limiting case:  $P = \varepsilon = a_0 n^2$ , corresponding

to the pure incompressible state. However, once the matter is governed by  $P = \varepsilon$ , then the chemical potential  $\mu$  must achieve a universal maximum, *i.e.*  $\frac{\partial \mu}{\partial n} = 0$ .

✧ Based on thermodynamical considerations, it was shown in [2] that at  $\rho = \rho_{crit} \approx 3 \times \rho_0$ , in combination with zero-entropy condition, the Gibbs function attains a global zero-minimum, thereby facilitating a crossover phase transition into a globally confined gluon-quark superfluid, where  $\frac{\partial \mu}{\partial n} = 0$ .

- The formation of incompressible gluon-quark superfluids is associated with energy enhancement of the gluon field at the surface of the core, which is needed for globally re-confining the enclosed quarks, thereby effectively enhancing the effective mass of the core.
- The phase transition of the quantum fluid in the BL from compressible-dissipative into incompressible superfluid states is associated with changes of the spacetime topology from a curved spacetime into a purely flat one. The latter reaction is due to causality, which prohibits incompressible superfluids to be embedded by a curved spacetime. Indeed, the topology change of spacetime is associated with the emission of gravitational waves. However, due to the tiny little volume of the BL, the detection of GW-emission during glitch-events would be much below the sensitivity of today GW-detectors.
- Both the phase transition of matter and the topological change of spacetime in the boundary layer can be provoked by the strong nuclear force (SNF) only, which appears to develop into a macroscopic force as the pulsars ages.

In fact, as the core is made of SuSu-matter, the core is equivalent to a super-baryon, in which the enclosed quarks are shielded by a gluon cloud [23]. As it will be shown later, the SNF transmitted by this cloud is found to correlate nicely with the size and mass of the core. The neutrons in the BL become increasingly locked to the core, thereby gradually adapting the physical conditions of the matter inside the core.

Following the scenario of [22], the occurrence of glitches in pulsars follows a well defined sequence, whose elements are  $\{\alpha_c^n\}$  where  $\alpha_c^n = \Omega_c^n / \Omega_c^{n+1} = 1 + (\Delta\Omega / \Omega)^n$ , and  $n : 0 \rightarrow \infty$ . Here  $n = 0$  corresponds to the first glitch event immediately after the pulsar's formation, whereas  $n = \infty$  corresponds to the final glitch event at the end of the pulsar's luminous lifetime.

Thereupon, let  $R_n, \Omega_n$  be respectively the radius and angular frequency of the SuSu-core at the verge of the glitch event number "n". The rotational energies of the SuSu-core at time  $t_n$  and  $t_{n+1}$  read:

$$E_{rot,SB}^n = \frac{4\pi\rho_{crit}}{15} R_n^5 \Omega_n^2$$

$$E_{rot,SB}^{n+1} = \frac{4\pi\rho_{crit}}{15} R_{n+1}^5 \Omega_{n+1}^2.$$

From the conservation of rotational energy:  $E_{rot,SB}^n = E_{rot,SB}^{n+1}$ , we obtain the relation:

$$\left(\frac{R_{n+1}}{R_n}\right)^5 = \left(\frac{\Omega_n}{\Omega_{n+1}}\right)^2. \tag{8}$$

Inserting  $R_{n+1} = R_n + \delta R_n^{BL}$ ,  $\Omega_n = \Omega_{n+1} + \delta \Omega_n$  and using Taylor-expansion, then the width of the boundary layer (BL) would correlate as follows:

$$\frac{\delta R_n^{BL}}{R_n} \approx \frac{2}{5} \frac{\delta \Omega_n}{\Omega_n}. \tag{9}$$

$\delta R_n^{BL}, \delta \Omega_n$  here denote the width of the boundary layer between the Su-Su-core and the ambient dissipative medium and the absolute difference between the rotational frequencies of the core before and after the glitch event, respectively.

Based thereon, the width of the BL during different evolutionary epochs of the pulsar may be estimated as follows:

$$\frac{\delta R_{BL}^n}{R_{SB}^n} \approx \begin{cases} \leq 1.4 \times 10^{-10} & \tau_{age} = 0 \\ 2.2 \times 10^{-8} & \tau_{age} = 1000 \text{ yrs/Crab} \\ 1.6 \times 10^{-6} & \tau_{age} = 10000 \text{ yrs/Vela} \\ 3.8 \times 10^{-6} & \tau_{age} = 10 \text{ Myr} \end{cases} \tag{10}$$

where  $\tau_{age}$  stands for the age of the pulsar, provided the object is perfectly isolated and shielded from whatsoever external effects. In calculating the ratio at  $\tau_{age} = 0$ , the initial values  $\alpha_c^{(n=0)} = 3.5 \times 10^{-10}$ ,  $\Omega^{(n=0)} = 1400/\text{s}$  and  $B^{(n=0)} = 10^{13}$  Gauss have been used (see [24] for further details). The values at  $\tau_{age} = 1000, 10000 \text{ yrs}$  and  $\tau_{age} = 10 \text{ Myr}$  are chosen to enable partial comparison with observations of the glitch events of the Vela and Crab pulsars. On the other hand the numerical values of  $\alpha_c^{n,n+1}$  have been selected from the sequence  $\{\alpha_c^n\}$  displayed in **Figure 8** of [22].

For determining  $R_{SB}^n$  we use the current glitch-observation of the Vela and Crab and try to extrapolate them to other epochs. Based on Equations (13, 14, 15) in [22], the correlation of the inertia of the ambient dissipative media,  $I_{AM}$ , of the Crab and Vela pulsars reads:

$$I_{AM}^{Vela} \approx 10^{-2} I_{AM}^{Crab}, \tag{11}$$

whereas the requirement that the ejected rotational energy off the core of the Vela pulsar in the form of vortices to be observationally noticeable, implies that

$$\delta R_{SB}^{now,Vela} \geq 10^{-2} R_*^{Vela}. \text{ This implies that } \delta R_{SB}^{now,Vela} \approx \frac{5}{2} \delta R_{SB}^{now,Crab}.$$

Consequently, the cosmic values of  $R_{SB}^n$  can be summarized as follows:

$$\delta R_{SB}^n = \begin{cases} \mathcal{O}(10^{-7} \text{ cm}) & \tau_{age} = 0 \\ \mathcal{O}(10^{-4} \text{ cm}) & \tau_{age} = 1000 \text{ yrs/Crab} \\ \mathcal{O}(10^{-2} \text{ cm}) & \tau_{age} = 10000 \text{ yrs/Vela} \\ \mathcal{O}(1 \text{ cm}) & \tau_{age} = 10 \text{ Myr} \end{cases} \tag{12}$$

An urgent question here is:

What is the nature of force in the boundary layer that is capable of triggering glitches?

Here we argue that the SNF is the deriving force that is capable of changing instantly both the physical properties of the quantum fluid as well as the topology of spacetime in the BL.

- Following [22], the core mimics a super-baryon (SB), in which the enclosed quarks are shielded by a gluon-cloud. The medium inside the SB interacts with overlaying supranuclear dense neutrons via vector mesons: the messengers of the SNF. In turn, the SNF locks the neutrons gradually to the core and enforces them to rotate rigidly with the core.
- The SNF generally operates effectively on nuclear length scales, *i.e.* when  $\delta R_{BL}^n \approx R_{SB}^n = \mathcal{O}(1)$  fm. However, the inertia of a core having the neutron-size would be approximately 100 orders of magnitude smaller than that of the ambient medium. In this case, its rotational and thermal decoupling from the ambient medium would be almost impossible.

On the other hand, in order for a SuSu-core to survive and affect the dynamics of the ambient medium, its inertia must have a minimum critical value. Here we recall that the initial frequency of a newly born pulsar is approximately 1400/s [24]. In order for a SuSu-core to be able to eject one single vortex, its radius must be larger than  $10^3$  cm, hence its minimum mass:  $\mathcal{M}_{SB}^{l=0} \geq 2.58 \times 10^{24}$  g.

Indeed, the above tabulated values of  $\delta R_{BL}^n$  show that  $\delta R_{BL}^n$  correlates nicely with the size of the enclosed SuSu-core and it may even become of macroscopic size at the end of pulsars luminous lifetime.

- The next related question reads: What keeps the core dynamically stable against the weight of the overlying massive shells, or equivalently to be stable against further compression by the surrounding curved spacetime?

As the gravitational potential inside the core is constant, then the medium has zero stratification due to gravity. In this case the only opposing force against gravitational collapse is the pressure due to the uncertainty principle as well as the pressure jump across the interface between SuSu-cores and the ambient compressible dissipative medium. The medium in the BL is still fermionic and the governing pressure is due to the Pauli exclusion principle. Moreover, similar to the bag energy confining the quarks inside individual baryons, the dynamics across the surface of the SuSu-core may be dominated by an extraordinary strong surface tension that is capable of confining the ocean of quarks quarks as well as opposing further compression.

- As the neutron's density in the BL approaches the critical value,  $\rho_{crit}$ , and as the chemical potential becoming closer to the upper-limit,  $\mu_{cr}$ , the EOS should converge to  $P \rightarrow \varepsilon = a_0 \bar{n}^2$ , where  $\bar{n}$  is the number density.

This limiting EOS corresponds to purely incompressible fluids and therefore the topology of the embedding spacetime ought to change into purely flat spacetime. In this case, two instantaneous reactions in the BL are expected to occur (see **Figure 11** detailed description):

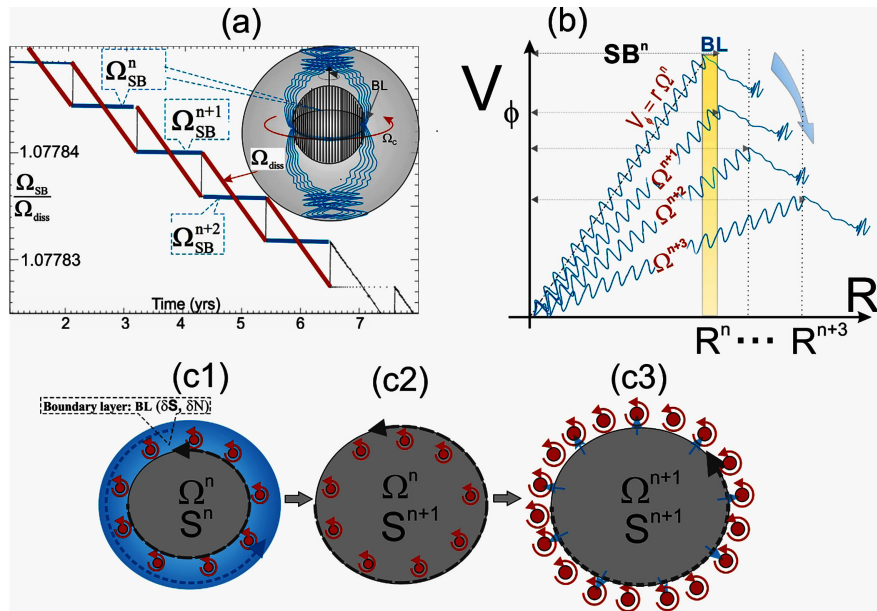


**Figure 11.** The three-stage glitch scenario. In (a) the time-development of both rotational frequencies of the SuSu-core (blue-color) and of the ambient medium (red-color) are shown, using GR-numerical calculations. In (b) the rigid-body rotation and increasing size of the SuSu-core for four successive glitch-events are shown. The boundary layer here has the width  $\delta R$ , area  $\delta S$  and contains  $\delta N$  vortices. In the lower panel we show the three-stage scenario of the glitch phenomena in pulsars. In (c1) the SuSu-core and boundary at the verge of a glitch event are shown. Once the SNF has locked the neutrons inside the BL, to the core and enforced them to adopt the same thermo- and hydrodynamical properties of the matter inside the core, then the spacetime embedding the BL undergoes a topological change into a flat spacetime and merges with that of the core (c2). However, once the resulting difference  $\Delta\Omega$  between  $\Omega_{SB}^n$  of the core and the ambient medium  $\Omega_{AM}^n$  has surpassed a critical value, then the core must undergo a transition into the next lower energy state by expelling a certain number of vortices (c3). In turn, the ambient medium absorbs the vortices and re-distributes them viscously, thereby giving rise to the prompt spin-up observed in glitching pulsars.

1) As the supranuclear dense matter in the BL becomes increasingly colder and its thermodynamical state and dynamics become indifferent from those of the matter inside the core, then it merges instantly with the core, thereby increasing its size and effective mass.

2) However, when  $\Delta\Omega = \Omega_n - \Omega_{n+1}$ , which measures the difference between the rotational frequency of the modified core and that of the matter at the base of the ambient medium, has surpassed a critical quantum value,  $\Delta\Omega_c$ , then the system undergoes a transition into the next lower energy state by promptly expelling a certain number of vortices into the ambient medium. The associated rotational energy will be absorbed and viscously re-distributed in the ambient medium. The corresponding time scale here is predicated to be of order:

$$\tau_{vis} = \frac{R_*^2}{\nu} = \mathcal{O}(1) \text{ s}, \tag{13}$$

where we have optimistically assumed that the viscous length scale is of order

$10^{-4}R_*$  and that the viscous interaction occurs at the frequency  $\Omega_{vis} = O(10^2) s^{-1}$ . This prediction agrees with observations of pulsars during glitch events [25].

- Based on the here-presented scenario, the mechanisms underlying the glitch phenomena in pulsars are due to dramatic changes of the physical conditions of the matter as well as of the topology of spacetime in the BL. Here the system operates on two different time scales: a relatively long times scale,  $\tau_{spin-down}$  and on the very short time scale,  $\tau_{quantum}$ .

During  $\tau_{spin-down}$ :

- The pulsar's crust spin-down due to the emission of magnetic dipole radiation almost in a continuous manner.

However as the crust is viscously coupled to the ambient dissipative and compressible medium in the shell overlying the SuSu-core, the matter in the whole shell must spin down in a similar manner, *i.e.*  $\dot{\Omega}_{AM} < 0$ .

- Cooling and spinning down of the matter in the shell enforces the supranuclear dense fluid at its base, *i.e.* in the BL, to adopt the physical and dynamical conditions of the SuSu-core almost in a continuous manner from inside-to-outside, facilitating a phase transition of the EOS into  $P = \varepsilon$ , *i.e.* into purely incompressible whilst changing the topology of the embedding spacetime into a purely flat one. As a consequence, the rotational frequency difference  $\delta\Omega^n = |\Omega_{BL} - \Omega_{AM}|$  becomes increasingly larger.

The above process provokes an instantaneous reaction of the SuSu-core: similar to superfluid Helium in a container, once  $\delta\Omega^n$  has surpassed the critical value  $\delta\Omega_{cr}^n$ , then the SuS-core reacts promptly: the BL then merges with the SuS-core, thereby triggering the core to make a transition into the next lower and quantum-mechanically permitted energy state by expelling a certain number of vortices.

$\tau_{quantum}$  may be predicted to be order  $\delta R_{BL}/V_s \leq 10^{-10} s$ .

- By the end of luminous lifetime of pulsars, the discrete repetition of mergers of the BL with SuSu-core should have metamorphosed the entire pulsars into a SuSu-object, thereby doubling its initial mass and reducing its radius to roughly coincide with the corresponding event horizon. For remote observers the object becomes practically invisible and therefore indistinguishable from stellar black holes.

The present evolutionary scenario may explain nicely, why neither black holes nor neutron stars have ever been observed in the mass range  $\{2.5\mathcal{M}_\odot \leq \mathcal{M} \leq 5\mathcal{M}_\odot\}$  as well as why the NS-merger GW170817 [4] did not collapse to form a stellar BH. If nature indeed forbids the formation of BHs in this mass regime, then our understanding of the big bang, the nature of dark matter and dark energy in cosmology should be revised (see [3] [26] for further details).

## Acknowledgements

The calculations have been carried out using the computer cluster of the IWR,

University of Heidelberg. We also thank Dr. Al-Marouf for reading the manuscript.

### Conflicts of Interest

The authors declare no conflicts of interest regarding the publication of this paper.

### References

- [1] Haensel, P., Potekhin, A.Y. and Yakovlev, D.G. (2007) *Neutron Stars 1*. Springer, Berlin. <https://doi.org/10.1007/978-0-387-47301-7>
- [2] Hujeirat, A.A. (2018) *Journal of Modern Physics*, **9**, 51-69. <https://doi.org/10.4236/jmp.2018.91004>
- [3] Hujeirat, A.A. (2018) *Journal of Modern Physics*, **9**, jmp.2018.94037.
- [4] Abbott, B.P., *et al.* (2017) *Physical Review Letters*, **119**, Article ID: 161101.
- [5] Miller, M.C. and Yunes, N. (2019) The New Frontier of Gravitational Waves. <https://doi.org/10.1038/s41586-019-1129-z>
- [6] Ozel, F. and Freire, P. (2016) *Annual Review of Astronomy and Astrophysics*, **54**, 401-440. <https://doi.org/10.1146/annurev-astro-081915-023322>
- [7] Espinoza, C.M., Lyne, A.G., Stappers, B.W. and Kramer, C. (2011) *Monthly Notices of the Royal Astronomical Society*, **414**, 1679-1704. <https://doi.org/10.1111/j.1365-2966.2011.18503.x>
- [8] Eya, I.O. and Urama, J.O. (2014) *International Journal of Astrophysics and Space Science*, **2**, 16.
- [9] Camenzind, M. (2007) *Compact Objects in Astrophysics*. Springer, Heidelberg.
- [10] Cook, G.B., Shapiro, S.L. and Teukolsky, S.A. (1994) *ApJ Letters*, **423**, L117. <https://doi.org/10.1086/187250>
- [11] Rajagopal, K. and Wilczek, F. (2000) *The Frontier of Particle Physics*, **3**, 2061-2151. [https://doi.org/10.1142/9789812810458\\_0043](https://doi.org/10.1142/9789812810458_0043)
- [12] Hujeirat, A.A. (2012) *Monthly Notices of the Royal Astronomical Society*, **423**, 2893-2900. <https://doi.org/10.1111/j.1365-2966.2012.21102.x>
- [13] Bethke, S. (2007) *Progress in Particle and Nuclear Physics*, **351**, 58.
- [14] Tanabashi, M., *et al.* (2018) *Physical Review D*, **98**, Article ID: 030001.
- [15] LHCb Collaboration (2015) *Physical Review Letters*, **115**, Article ID: 072001.
- [16] PHENIX Collaboration (2019) *Nature Physics*, **15**, 214-220. <https://doi.org/10.1038/s41567-018-0360-0>
- [17] Glendenning, N. (2007) *Special and General Relativity*. Springer, Berlin. <https://doi.org/10.1007/978-0-387-47109-9>
- [18] Hujeirat, A.A. and Thielemann, F.-K. (2009) *Monthly Notices of the Royal Astronomical Society*, **400**, 903-916. <https://doi.org/10.1111/j.1365-2966.2009.15498.x>
- [19] Yarmchuk, E.J., Gordon, M.J.V. and Packard, R.E. (1979) *Physical Review Letters*, **43**, 214. <https://doi.org/10.1103/PhysRevLett.43.214>
- [20] Walmsley, P.M., Golov, A.I., *et al.* (2007) *Physical Review Letters*, **99**, Article ID: 265302. <https://doi.org/10.1103/PhysRevLett.99.265302>
- [21] Fischer, M. and Hujeirat, A.A. (2019) Preprint, in Preparation.

- [22] Hujeirat, A.A. (2018) *Journal of Modern Physics*, **9**, jmp.2018.94038.
- [23] Witten, E. (1984) *Physical Review D*, **30**, 272.  
<https://doi.org/10.1103/PhysRevD.30.272>
- [24] Haensel, P., Lasota, J.P. and Zdunik, J.L. (1999) *AandA*, **344**, 151.
- [25] Ashton, G., Lasky, P.D., Graber, V. and Palfreyman, J. (2019) *Nature Astronomy*, **3**, 1143-1148. <https://doi.org/10.1038/s41550-019-0844-6>
- [26] Hujeirat, A.A. (2018) *Journal of Modern Physics*, **9**, 70-83.  
<https://doi.org/10.4236/jmp.2018.91005>